FULL PAPER

Dalton
www.rsc.org/dalton

Tuning the metal-to-metal charge transfer energy of cyano-bridged dinuclear complexes†

Paul V. Bernhardt,*[a] Fernando Bozoglian,[b] Brendan P. Macpherson[a] and Manuel Martinez[a]

[a] *Department of Chemistry, University of Queensland, Brisbane, 4072, Australia*

[b] *Departament de Química Inorgànica, Universitat de Barcelona, Martí i Franquès 1–11, 08028, Barcelona, Spain*

Received 12th May 2004, Accepted 18th June 2004
First published as an Advance Article on the web 21st July 2004

The metal-to-metal charge transfer (MMCT) transitions of a series of Class II mixed valence dinuclear complexes bearing cyano bridging ligands may be varied systematically by variations to either the hexacyanometallate(II) donor or Co^{III} acceptor moieties. Specifically, the new dinuclear species *trans*-$[L^{14S}CoNCFe(CN)_5]^-$ (L^{14S} = 6-methyl-1,11-diaza-4,8-dithia-cyclotetradecane-6-amine) and *trans*-$[L^{14}CoNCRu(CN)_5]^-$ (L^{14} = 6-methyl-1,4,8,11-tetraazacyclotetradecane-6-amine) have been prepared and their spectroscopic and electrochemical properties are compared with the relative *trans*-$[L^{14}CoNCFe(CN)_5]^-$. The crystal structures of Na{*trans*-$[L^{14S}CoNCFe(CN)_5]$}·5½H_2O·½EtOH, Na{*trans*-$[L^{14}CoNCRu(CN)_5]$}·3H_2O and Na{*trans*-$[L^{14}CoNCRu(CN)_5]$}·8H_2O are also reported. The ensuing changes to the MMCT energy have been examined within the framework of Hush theory, and it was found that the free energy change between the redox isomers was the dominant effect in altering the energy of the MMCT transition.

Introduction

In recent years we have reported the syntheses and characterisation of a new class of molecular mixed valence dinuclear complexes comprising ferrocyanide as the electron donor and Co^{III} as the electron acceptor.[1–4] As an example, the complex anion *trans*-$[L^{14}CoNCFe(CN)_5]^-$ (Chart 1) and its analogues fall into the Robin and Day[5] Class II group of mixed valence compounds, where weak to moderate electronic coupling between the metal centres is present and electronic transitions from the individual Co^{III} and Fe^{II} chromophores are apparent.

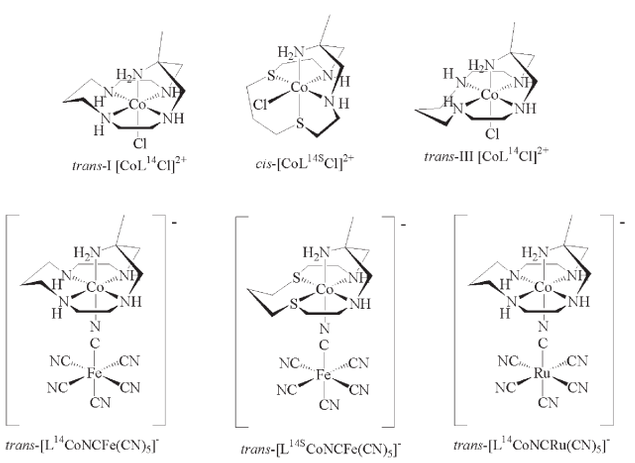

Chart 1

As such, compounds of this type are well described by Hush theory[6] and the energy of the metal-to-metal charge transfer (MMCT) transition (E_{op}, cm^{-1}) may be expected to follow eqn. (1)

$$E_{op} = \Delta G^o + \lambda \quad (1)$$

where ΔG^o is the free energy difference between the 'redox isomers' (Co^{III}–Fe^{II} and Co^{II}–Fe^{III}) and λ is the combined outer and inner sphere reorganisational energy; effectively the excess vibrational energy that the MMCT excited state possesses following electronic excitation. The free energy difference (in units of cm^{-1}) may be approximated from the difference between the donor ($Fe^{III/II}$) and acceptor ($Co^{III/II}$) redox potentials *i.e.* $\Delta E^oF/11.97$ while the reorganisational energy can be approximated from the MMCT transition bandwidth at half height, $\Delta\bar{\nu}_{½}$ (cm^{-1}) according to eqn. (2)

$$\lambda = \Delta\bar{\nu}_{½}^2/2310 \text{ (at 300 K)} \quad (2)$$

Under favourable circumstances *i.e.* reversible electrochemistry and clearly resolved MMCT spectral bands, all three terms of eqn. (1) may be determined independently, which not only provides a rigorous test of the applicability of Hush theory to these compounds but also allows the two independent contributions of E_{op} to be determined and to understand the important factors that affect their magnitudes. Previously, we found that the influence of geometric isomerism on the MMCT energy of the closely related compounds *trans*-$[L^{14}CoNCFe(CN)_5]^-$ and *cis*-$[L^{14}CoNCFe(CN)_5]^-$ led to differences in both ΔG^o and λ.[3] However, as these changes were opposite in sign, the overall MMCT energies of the isomers were essentially the same. Earlier we had also found that changing the macrocyclic ring size from fourteen (*trans*-$[L^{14}CoNCFe(CN)_5]^-$) to fifteen gave essentially the same values of all three parameters.[2]

It has now become apparent to us that significant changes to the energy of E_{op}, and hence the colour of the complex, demand more forceful changes to the complex than simply changing macrocyclic ring size or its mode of binding (*trans* or *cis*). To this end, we report here two approaches to tuning the MMCT energy of *trans*-$[L^{14}CoNCFe(CN)_5]^-$, which involve replacing two of the secondary amines by thioethers (*trans*-$[L^{14S}CoNCFe(CN)_5]^-$) or by substituting Fe^{II} with Ru^{II} (*trans*-$[L^{14}CoNCRu(CN)_5]^-$). As we shall illustrate, the resulting dinuclear complexes exhibit quite different MMCT energies from their parent *trans*-$[L^{14}CoNCFe(CN)_5]^-$ complex and the application of Hush theory to these complexes has enabled a study of the effects on both ΔG^o and λ that are brought about by these changes to the donor and acceptor moieties of these unusual molecules.

Experimental

Syntheses

$K_4[Ru(CN)_6]$ was prepared as described.[7] The complexes *cis*-$[CoL^{14S}Cl](ClO_4)_2$[8] and *trans*-I $[CoL^{14}Cl](ClO_4)_2$·2H_2O[2] were prepared according to previously reported methods. All other reagents were obtained commercially and used without further purification.

† Electronic supplementary information (ESI) available: Figs. S1–S5. See http://www.rsc.org/suppdata/dt/b4/b407185a/

DOI: 10.1039/b407185a

Na{*trans*-[L^{14S}CoNCFe(CN)$_5$]}·8H$_2$O. A solution of of *cis*-[CoL^{14S}Cl](ClO$_4$)$_2$ (1 mmol) in water (100 cm^3) was adjusted to pH 6 with NaOH. To this was added K$_4$[Fe(CN)$_6$]·3H$_2$O (1 mmol) dissolved in water. The solution darkened in colour after *ca.* 15 min, and was then heated at 60 °C for a further 16 h. The resulting mixture was filtered, diluted to *ca.* 2 dm^3 and passed through a Sephadex C-25 cation exchange column (3 × 25 cm) to remove any cationic impurities. The desired (anionic) complex was not retained by the resin and the eluate was then adsorbed onto a Sephadex DEAE A-25 anion exchange column (2 × 40 cm; ClO_4^- form). The product was eluted with NaClO$_4$ solution (0.1 M) and reduced in volume to *ca.* 20 mL on a rotary evaporator (*caution*—perchlorate salts are potentially explosive and should never be taken to dryness on a rotary evaporator). A purple solid was obtained by cooling the concentrated solution in a refrigerator (36% yield). Anal. found C, 28.9; H, 5.6; N, 18.2% (Calcd for C$_{17}$H$_{41}$CoFeN$_9$NaO$_8$S$_2$ requires C, 29.1; H, 5.9; N, 18.0%). Electronic spectrum (H$_2$O): λ_{max} 566 nm (ε = 515 dm^3 mol^{-1} cm^{-1}), 462 (507). NMR: (^{1}H, D$_2$O) 1.28 (s, –CH$_3$), 1.75–2.05 (m, –CH$_2$–), 2.65–3.6 (m, –CH$_2$–), 3.9–4.0 ppm (d of t, –CH$_2$–); (^{13}C, D$_2$O) 21.8, 28.1, 34.5, 44.0, 58.4, 64.1, 71.6, 176.5, 177.1, 194.8 ppm. IR (KBr disc): $\bar{\nu}_{CN}$ peaks (cm^{-1}) 2040 (s, equatorial CN), 2079 (m, axial CN), 2122 (m, μ-CN). X-ray quality crystals were obtained by vapour diffusion of ethanol into a concentrated aqueous solution of the complex.

Na{*trans*-[L^{14}CoNCRu(CN)$_5$]}·4H$_2$O. The complex *trans*-[CoL^{14}Cl](ClO$_4$)$_2$ (1 mmol) was first converted to its hydroxo form by stirring a solution of the complex at *ca.* pH 10 at room temperature for 10 min. Base hydrolysis was apparent from a colour change from red to apricot. The pH was then lowered to *ca.* 5 with HCl to afford the more reactive aqua complex (orange) and an equimolar amount of K$_4$[Ru(CN)$_6$] (1 mmol), dissolved in a minimum amount of water, was added to the solution. The pH of the mixture was monitored and kept above 6 at all times to avoid the precipitation of an orange powder (typically at pH 5), which, if formed, could be redissolved on addition of base. The orange solution was stirred at 60 °C for 16 h, filtered, diluted ten-fold, and then passed through a Sephadex C-25 cation exchange column to remove cationic species. The desired complex, was not retained by the resin, but was collected and the column washed with a further 500 ml of water. The eluate was adsorbed onto a Sephadex DEAE A-25 anion exchange column and eluted with 0.1 M NaClO$_4$ as a single band. Orange power formed from the concentrated solution upon standing (38% yield). Anal. found C, 31.6; H, 5.3; N, 24.2%. Cald for C$_{17}$H$_{35}$CoN$_{11}$NaO$_4$Ru requires C, 31.9; H, 5.5; N, 24.1%. Electronic spectrum (H$_2$O): λ_{max} 472 nm (ε = 314 dm^3 mol^{-1} cm^{-1}), 382 (712). NMR: (^{1}H, D$_2$O/TSP) 1.40 (s, –CH$_3$), 1.80–3.60 (m, –CH$_2$–) ppm; (^{13}C, D$_2$O/TSP) 20.9, 30.7, 52.9, 54.9, 55.1, 62.1, 68.5, 162.5, 163.9, 179.6 ppm. Infrared: $\bar{\nu}_{CN}$ peaks (cm^{-1}) 2049 (s, equatorial CN), 2083 (m, axial CN), 2123 (m, μ-CN).

X-ray quality crystals were obtained by vapour diffusion of ethanol into a concentrated aqueous solution of the complex. Crystals of two different hydrates of the complex were observed to form simultaneously, and could be separated by hand on the basis of their morphology. Crystals of Na{*trans*-[L^{14}CoNCRu(CN)$_5$]}·3H$_2$O were much larger and darker than Na{*trans*-[L^{14}CoNCRu(CN)$_5$]}·8H$_2$O. Both sets of crystals exhibited identical solution behaviour.

Physical methods

Electronic spectra were recorded on a Perkin-Elmer Lambda 40 spectrophotometer, and infrared spectra were obtained on a Perkin-Elmer 1600 Series FTIR spectrometer, with samples dispersed in KBr discs. Nuclear magnetic resonance spectra were recorded at 200 (^{1}H) and 50.3 MHz (^{13}C) on a Bruker AC200 spectrometer using D$_2$O as the solvent and sodium(trimethylsilyl)-propionate (TSP) as the reference. A BAS100B/W potentiostat was used for all electrochemistry experiments. Cyclic voltammetry was performed with either a glassy-carbon working electrode or a PARC 303 model static mercury-drop electrode, employing a Pt-wire auxiliary electrode and a Ag/AgCl reference electrode. All aqueous solutions for electrochemistry contained *ca.* 2 mmol dm^{-3} analyte and 0.1 mol dm^{-3} NaClO$_4$ and were purged with nitrogen gas before measurement. Pulse radiolysis experiments were performed on 0.1 mmol dm^{-3} solutions of the compounds dissolved in Millipore water. The experimental setup has been described previously.[2]

Crystallography

Cell constants were determined for all complexes by least-squares fits to the setting parameters of 25 independent reflections measured on an Enraf-Nonius CAD4 four-circle diffractometer employing graphite-monochromated Mo Kα radiation (0.71073 Å) and operating in the ω–2θ Å scan mode. Data reduction and empirical absorption correction (ψ-scans) were performed with the WinGX package.[9] Structures were solved by direct methods with SHELXS and refined by full-matrix least-squares analysis with SHELXL-97.[10] The H atoms of noncoordinated water molecules were not modeled. Due to the large number of variables relative to observed reflections, the C-atoms in Na{*trans*-[L^{14S}CoNCFe(CN)$_5$]}·5½H$_2$O·½EtOH and the O-atoms in Na{*trans*-[L^{14}CoNCRu(CN)$_5$]}·8H$_2$O were modeled isotropically. Drawings of the molecules were produced with ORTEP3.[11] Crystal instability proved problematic for Na{*trans*-[L^{14S}CoNCFe(CN)$_5$]}·5½H$_2$O·½EtOH. Despite several attempts, only 84% of a unique data set (to 2θ = 50°) could be obtained. Low temperature (*ca.* 150 K) X-ray analysis merely resulted in immediate loss of all diffraction intensity. Nevertheless, this partial data set enabled structure solution and partial anisotropic refinement to a precision that was satisfactory, although not ideal. The structure of Na{*trans*-[L^{14}CoNCRu(CN)$_5$]}·8H$_2$O suffered from absorption effects that could not be adequately accounted for by empirical (psi-scan) absorption correction. This left peaks of *ca.* 3 e Å^{-3} adjacent to each Ru atom and the final precision of the structure was affected somewhat.

Crystal data

Na{*trans*-[L^{14S}CoNCFe(CN)$_5$]}·5½H$_2$O·½EtOH C$_{18}$H$_{39}$CoFeN$_9$NaO$_6$S$_2$, M = 677.46, monoclinic, a = 23.23(2), b = 19.473(6), c = 15.606(9) Å, β = 123.53(4)°. U = 5885(6) Å^3, D_c = 1.529 g cm^{-3}, T = 296 K, space group $C2/c$ (No. 15), Z = 8, μ(Mo Kα) = 12.62 cm^{-1}, 4379 unique reflections measured (R_{int} = 0.0620), R_1 = 0.1028, wR_2 = 0.3434 (all data).

Na{*trans*-[L^{14}CoNCRu(CN)$_5$]}·3H$_2$O. C$_{17}$H$_{33}$CoN$_{11}$NaO$_3$Ru, M = 622.53, orthorhombic, a = 9.6244(5), b = 15.353(2), c = 16.389(2) Å, U = 2421.7(5) Å^3, D_c = 1.707 g cm^{-3}, T = 296 K, space group $P2_12_12_1$ (No. 19), Z = 4, μ(Mo Kα) = 13.70 cm^{-1}, 2426 (unique) reflections measured (R_{int} = 0), R_1 = 0.0404, wR_2 = 0.1003 (all data).

Na{*trans*-[L^{14}CoNCRu(CN)$_5$]}·8H$_2$O. C$_{17}$H$_{43}$CoN$_{11}$NaO$_8$Ru, M = 712.61, monoclinic, a = 15.509(5), b = 20.039(7), c = 20.04(3) Å, β = 91.14(9)°, U = 6227(1) Å^3, D_c 1.520 g cm^{-3}, T = 296 K, space group $P2_1/c$ (No. 14), Z = 8, μ(Mo Kα) = 10.87 cm^{-1}, 10957 unique reflections (R_{int} = 0.1723), R_1 = 0.0911, wR_2 = 0.2885 (all data).

CCDC reference numbers 238538–238540.

See http://www.rsc.org/suppdata/dt/b4/b407185a/ for crystallographic data in CIF or other electronic format.

Results and discussion

The syntheses of the Co^{III}–Fe^{II} and Co^{III}–Ru^{II} complexes were straightforward and involved ligand substitution by the hexacyanometallate anion at the coordination site vacated by the chloro ligand of the macrocyclic cobalt precursor. Yet, the two syntheses are subtly different. It is now well established from several kinetic studies[12–15] that the formation of complexes of the type [LCoNCFe(CN)$_5$]$^-$ (L represents a pentadentate coordinated ligand or five monodentate ligands) proceeds by a mechanism that involves, as an intermediate step, outer sphere (Fe^{II} to Co^{III}) electron transfer to form a labile Co^{II} intermediate which undergoes rapid ligand substitution by ferrocyanide. A similar mechanism appears to occur during the formation of *trans*-[L^{14S}CoNCFe(CN)$_5$]$^-$, as there is a rapid colour change of the solution following mixing the

mononuclear precursors, but not *trans*-$[L^{14}CoNCRu(CN)_5]^-$, which forms much more slowly. The most significant difference here is between the redox potentials of the hexacyanometallate complexes; the Ru analogue being some 600 mV more positive than its Fe relative. Evidently, $[Ru(CN)_6]^{4-}$ is too poor a reductant to produce any significant amount of the Co^{II} complex of L^{14S} and the reaction must take place directly without catalysis by electron transfer.

The infrared spectra of both complexes as KBr discs reveal three separate sets of $\bar{\nu}_{CN}$ vibrations at ~2045, ~2080 and ~2125 cm^{-1}, and these bands were assigned by reference to previous vibrational spectroscopic studies on complexes comprising both bridging and terminally bound cyano ligands.[16,17] The four equatorial cyanides appear at lowest frequency and are most intense, the axial cyanide *trans* to the bridging ligand appears in the middle and the bridging cyano ligand vibration emerges at highest frequency. It is notable that the two complexes give essentially the same CN^- vibrational frequencies despite the central metal of the two hexacyanometallate moieties being different. The reason that the bridging cyano ligand vibrates at a higher frequency than the terminal ligands may be attributed to stabilisation of the (occupied) σ_{2S}* antibonding orbital of the bridging CN^- ligand through overlap with the Co orbitals, thus strengthening the CN bond.

The pentadentate macrocycles L^{14} and L^{14S} have been identified in a variety of geometric (*trans*/*cis*) and N-based diastereomeric forms when complexed with Co^{III}.[2,8,18–22] However, both *trans*-$[L^{14S}CoNCFe(CN)_5]^-$ and *trans*-$[L^{14}CoNCRu(CN)_5]^-$ exhibit NMR spectra consistent with mirror plane symmetry, which can only be present when the macrocycles adopt a conformation where the pendent amine is *trans* to the bridging cyano ligand. Interestingly, *trans*-$[L^{14S}CoNCFe(CN)_5]^-$ forms exclusively from *cis*-$[CoL^{14S}Cl]^{2+}$ (or an unpurified isomeric mixture of *cis*- and *trans*-$[CoL^{14S}Cl]^{2+}$). In contrast, we previously reported[3] that *cis*-$[L^{14}CoNCFe(CN)_5]^-$ may be synthesised from *cis*-$[CoL^{14}Cl]^{2+}$ without significant isomerisation. The driving force for this isomerisation (from *cis*-$[CoL^{14S}Cl]^{2+}$ to *trans*-$[L^{14S}CoNCFe(CN)_5]^-$) is unclear. A comprehensive mechanistic study of the *cis*–*trans* isomerisation reactions of mononuclear macrocyclic Co^{III} complexes from this series is currently underway and this may provide a clearer picture of the differences we have observed in the coordination chemistry of the pentaamine (L^{14}) and triamine–dithioether (L^{14S}) ligands.

NMR spectroscopy could not resolve the absolute stereochemistry of the donor atoms in *trans*-$[L^{14S}CoNCFe(CN)_5]^-$ or *trans*-$[L^{14}CoNCRu(CN)_5]^-$. As illustrated in Chart 1, the so-called *trans*-I (all secondary amine H-atoms/S-donor lone pairs on the same side of the macrocyclic plane) and *trans*-III (two up and two down) isomers possess the same symmetry. Indeed *trans*-$[CoL^{14}Cl]^{2+}$ has been isolated in both its *trans*-I[2,22] and *trans*-III forms[19] (as well as its *cis* isomer[18,22]), as confirmed by X-ray crystallography.

The crystal structure of Na{*trans*-$[L^{14S}CoNCFe(CN)_5]$}·5½-H_2O·½EtOH was determined and a view of the complex anion is shown in Fig. 1. Although only a partial data set could be obtained, the structure was solved and refined without problems, albeit to a poorer precision than one would like. The pendent amine coordinated to the Co ion is *trans* to the bridging cyano ligand, as expected from the NMR data. The two five-membered chelate rings have the same chirality *i.e.* they adopt a staggered relative conformation and the six-membered chelate ring adopts a chair conformation, but with the S-donor lone pairs above the macrocyclic plane as drawn, which defines a *trans*-III configuration. The shortest bond to the Co ion is the N-bound cyano ligand and the longest ones are to the S-donors. The Co–N(amine) and Co–S bond lengths are similar to those seen in the structures of *cis*-$[CoL^{14S}Cl]^{2+}$ and *cis*-$[CoL^{14S}(OAc)]^{2+}$.[8,20] The Fe–C coordinate bonds around the ferrocyanide moiety are as expected,[23] and the bond angles define an approximately octahedral coordination geometry. The bridging Co–N–C–Fe moiety is close to linear and the Co–Fe separation is about 4.90 Å. The sodium counter ion (not shown) is in an N_2O_2 distorted tetrahedral coordination environment comprising two water molecules and two terminal cyano ligands from different complex anions. The asymmetric unit includes five water molecules (one of them disordered over two sites), and a disordered water/ethanol solvent molecule; both contributors refined to half occupancy.

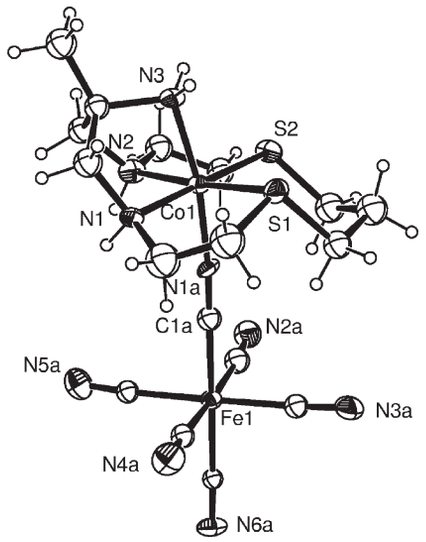

Fig. 1 ORTEP drawing of the *trans*-$[L^{14S}CoNCFe(CN)_5]^-$ anion (30% probability ellipsoids). Selected bond lengths (Å): Co(1)–N(1A) 1.86(1); Co(1)–N(1) 1.97(1); Co(1)–N(2) 1.98(1); Co(1)–N(3) 1.93(1); Co(1)–S(1) 2.206(5), Co(1)–S(2) 2.219(6); Fe–C 1.88(2)–1.94(2).

Two different crystal forms of Na{*trans*-$[L^{14}CoNCRu(CN)_5]$} (a trihydrate and an octahydrate) were identified. In Na{*trans*-$[L^{14}CoNCRu(CN)_5]$}·$3H_2O$ the coordination environment of the macrocyclic Co^{III} centre (Fig. 2, left) is *trans*-I, as seen before in the structures of Na{*trans*-$[L^{14}CoNCFe(CN)_5]$}·$8H_2O$ and its ferric analogue *trans*-$[L^{14}CoNCFe(CN)_5]$.[2,3] In fact the *trans*-I N-based diastereomeric form has been seen in all but one structurally characterised, pentadentate-coordinated Co^{III} complex of L^{14}.[21,22] The coordinate bonds around the Ru atom are the same within experimental error and consistent with those found in other hexacyanoruthenate(II) containing structures.[24–26] A notable feature is the pronounced distortion of the C1a–N1a–Co angle (162.8(8)°) from its ideally linear value. Examination of the crystal packing (ESI Fig S1†) illustrates that this distortion can be attributed to repulsion between the Co pentaamine fragment and the tetrahedrally coordinated Na atom (which is also coordinated to the cyano ligand through N4a).

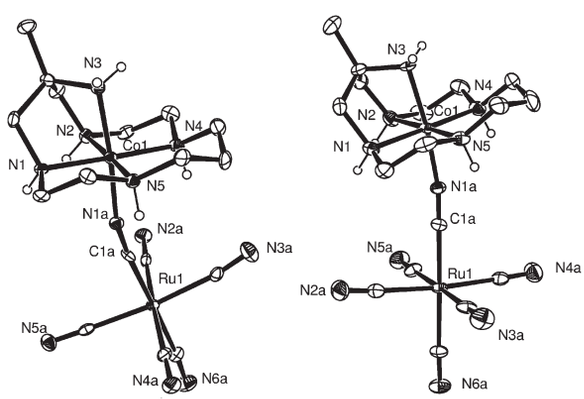

Fig. 2 ORTEP drawings of the *trans*-$[L^{14}CoNCRu(CN)_5]^-$ complex anions (30% probability ellipsoids) from Na{*trans*-$[L^{14}CoNCRu(CN)_5]$}·$3H_2O$ (left): selected bond lengths (Å) Co(1)–N(1A) 1.910(7); Co(1)–N(1) 1.941(7); Co(1)–N(2) 1.967(9); Co(1)–N(3) 1.952(7); Co(1)–N(4) 1.966(7); Co(1)–N(5) 1.958(8); Ru(1)–C 1.996(8)–2.052(9) and Na{*trans*-$[L^{14}CoNCRu(CN)_5]$}·$8H_2O$ (right, one of two crystallographically independent molecules shown. No significant differences between coordinate bond lengths of octahydrate and trihydrate structure). Alkyl H-atoms omitted for clarity.

The structure of Na{*trans*-$[L^{14}CoNCRu(CN)_5]$}·$8H_2O$ is isomorphous with the previously reported[2] Na{*trans*-$[L^{14}CoNCFe(CN)_5]$}·$8H_2O$ and contains two independent formula

units within the asymmetric unit. Both independent complex anions have similar conformations and coordinate bond lengths; one of these is shown in Fig. 2 (right). Given that the structure of the isomorphous Co^{III}–Fe^{II} analogue has been discussed before,[2] the discussion will be brief. The most notable feature in comparison with the trihydrate structure is that the distortion of the C1a–N1a–Co angle (171(1)°) is less severe in this case. The configuration of the secondary amine N-donors is again *trans*-I.

Cyclic voltammetry experiments of *trans*-$[L^{14S}CoNCFe(CN)_5]^-$ and *trans*-$[L^{14}CoNCRu(CN)_5]^-$ were carried out under identical conditions in order to accurately determine the redox potentials of the donor and acceptor centres. The voltammograms are presented in Fig. 3 alongside that of *trans*-$[L^{14}CoNCFe(CN)_5]^-$, reported previously,[2] for comparison. Totally reversible $Co^{III/II}$ and $Fe^{III/II}$ or $Ru^{III/II}$ couples are apparent in all cases. The *trans*-$[L^{14S}CoNCFe(CN)_5]^-$ complex (Fig. 3(b)) exhibits an anodically shifted $Co^{III/II}$ wave (~200 mV) relative to the pentaamine analogue *trans*-$[L^{14}CoNCFe(CN)_5]^-$ (Fig. 3(a)). This may be attributed to the softer thioether donors stabilizing the divalent oxidation state relative to its pentaamine macrocyclic relative. The $Fe^{III/II}$ couples are the same, as expected.

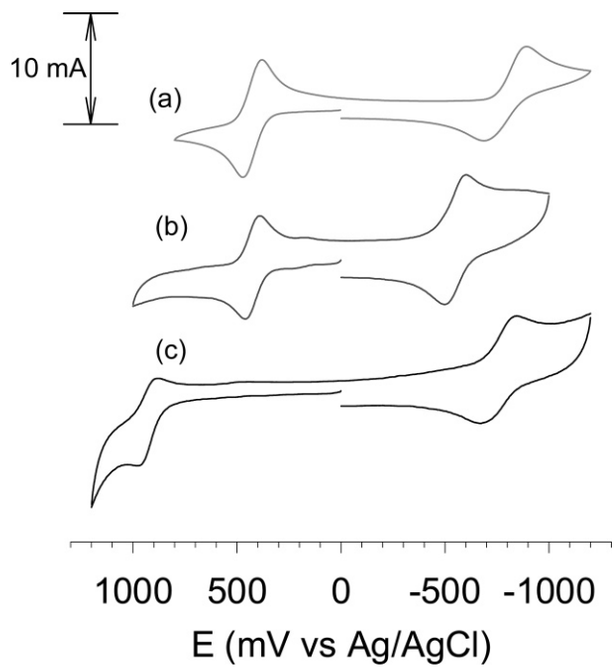

Fig. 3 Cyclic voltammograms of (a) *trans*-$[L^{14}CoNCFe(CN)_5]^-$, (b) *trans*-$[L^{14S}CoNCFe(CN)_5]^-$ and (c) *trans*-$[L^{14}CoNCRu(CN)_5]^-$. All complexes *ca.* 5 mmol dm^{-3} (supporting electrolyte 0.1 mol dm^{-3} $NaClO_4$), scan rate 100 mV s^{-1}, glassy carbon working electrode. Each cycle was initiated in the anodic direction.

Changing the hexacyanometallate moiety, while retaining the same Co^{III} macrocyclic complex unit has a much greater influence on the electrochemistry. The difference between the higher potential $Fe^{III/II}$ (Fig. 3(a)) and $Ru^{III/II}$ (Fig. 3(c)) couples is striking (~500 mV) and similar to the difference found between redox potentials of the mononuclear $[Ru(CN)_6]^{3-/4-}$ and $[Fe(CN)_6]^{3-/4-}$ precursors.

The optical spectra of *trans*-$[L^{14S}CoNCFe(CN)_5]^-$, *trans*-$[L^{14}CoNCRu(CN)_5]^-$, and *trans*-$[L^{14}CoNCFe(CN)_5]^-$ (reported previously[2]) are shown in Fig. 4. Arrows highlight the MMCT transitions. In each case, d–d bands characteristic of the appropriate Co^{III} chromophore are apparent around 450 nm, although spectral overlap with the MMCT transition is evident. The $[Ru(CN)_6]^{4-}$ chromophore of *trans*-$[L^{14}CoNCRu(CN)_5]^-$ exhibits no absorption bands in the spectral range shown whereas the lowest energy transition of ferrocyanide appears at about 330 nm and is clearly seen in the spectrum of *trans*-$[L^{14}CoNCFe(CN)_5]^-$ (Fig. 4(a)). In the spectrum of *trans*-$[L^{14S}CoNCFe(CN)_5]^-$, a shoulder is apparent at a wavelength consistent with the ferrocyanide chromophore but its absorbance maximum is obscured by a more intense ligand to metal (S → Co^{III}) charge transfer transition. The energies of the three MMCT transitions are well separated and result in the vastly different colours of *trans*-$[L^{14S}CoNCFe(CN)_5]^-$ (purple), *trans*-$[L^{14}CoNCRu(CN)_5]^-$ (orange) and *trans*-$[L^{14}CoNCFe(CN)_5]^-$ (maroon).

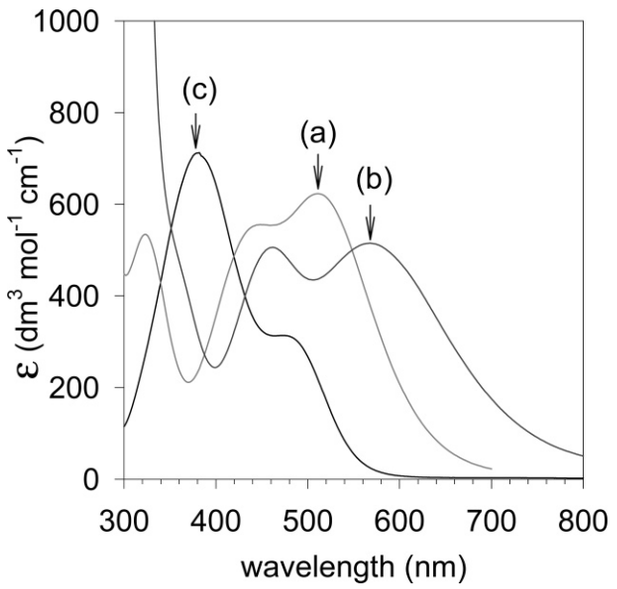

Fig. 4 UV-visible spectra (H_2O) of (a) trans-$[L^{14}CoNCFe(CN)_5]^-$ (b) trans-$[L^{14S}CoNCFe(CN)_5]^-$ and (c) trans-$[L^{14}CoNCRu(CN)_5]^-$. The MMCT transition is highlighted with an arrow.

Oxidation of *trans*-$[L^{14S}CoNCFe(CN)_5]^-$ to the ferric analogue *trans*-$[L^{14S}CoNCFe(CN)_5]$ could be achieved with $S_2O_8^{2-}$. The MMCT transition at 568 nm vanishes and a more intense band around 400 nm, consistent with the $[Fe(CN)_6]^{3-}$ chromophore, emerges (ESI Fig. S3†). Isosbestic points were apparent and indicative of only two absorbing species being present throughout the course of the reaction. The particularly high potential $Ru^{III/II}$ redox couple complicated a similar chemical oxidation experiment with *trans*-$[L^{14}CoNCRu(CN)_5]^-$. Therefore, electrochemical oxidation was employed using bulk electrolysis, with the working electrode poised at 1100 mV *vs.* Ag/AgCl. The resulting spectrum of the oxidised product (ESI Fig. S4†) resembles that of the starting material, but there are significant differences. A broader band with similar intensity replaces the MMCT maximum. A similar spectrum was found when pulse radiolytically generated hydroxyl radicals were employed as the oxidant (ESI Fig. S4†). The spectrum of $[Ru(CN)_6]^{3-}$ exhibits three intense broad absorption bands from 250–370 nm ($\varepsilon = 1.5–2.0 \times 10^3$ dm^3 mol^{-1} cm^{-1})[27,28] and a smaller band with a maximum at 460 nm ($\varepsilon \sim 1000$ dm^3 mol^{-1} cm^{-1}). As expected, the MMCT transition of *trans*-$[L^{14}CoNCRu(CN)_5]^-$ vanishes upon oxidation, but is replaced by a new band from the Ru^{III} chromophore in the same region; thus the spectra of *trans*-$[L^{14}CoNCRu(CN)_5]^-$ and *trans*-$[L^{14}CoNCRu(CN)_5]$ are, coincidentally, very similar.

The MMCT transition of both complexes also vanishes upon reduction of the Co^{III} centre. In this case, the lability and air-sensitivity of the putative Co^{II}–M^{II} (M = Fe or Ru) complexes necessitated the rapid acquisition of an electronic spectrum following reduction. Pulse radiolytically generated aquated electrons were the reducing source of an N_2-purged solution of the Co^{III}–M^{II} (M = Fe or Ru) complex. In both complexes (ESI Fig. S5†), the MMCT transition is lost immediately following the pulse to generate a 'stable' fully reduced species, as no subsequent change in either absorption spectrum was seen over a period of a few seconds (the limit of the experimental setup). For *trans*-$[L^{14}CoNCRu(CN)_5]^{2-}$, all visible absorption bands (MMCT and Co^{III} d–d bands) vanish upon reduction. Significantly, the spectrum of reduced *trans*-$[L^{14S}CoNCFe(CN)_5]^{2-}$ is different from that of its pentaamminecobalt(II) relatives $[L^{14}CoNCFe(CN)_5]^{2-}$ and $[L^{14}CoNCRu(CN)_5]^{2-}$, with a prominent absorption band emerging at 450 nm (ε ~600 dm^3 mol^{-1} cm^{-1}). All known hexaaminecobalt(II) complexes are high spin, but the successive introduction of S-donors

Table 1 Spectroscopic and electrochemical data and calculated parameters in eqn. (1)

	E_{op}/cm^{-1}	$M^{III/II}(CN)_6$/mV[a]	$Co^{III/II}$/mV[a]	ΔG^o/cm^{-1})[b]	λ/cm^{-1}[c]	$\Delta\bar{\nu}_{1/2,app}$/cm^{-1}[d]	λ_{app}/cm^{-1}[e]
trans-[L^{14}CoNCFe(CN)$_5$]$^-$	**19 600**	425	−791	**9 800**	**9 800**	*4 700*	*9 600*
trans-[L^{14S}CoNCFe(CN)$_5$]$^-$	**17 500**	425	−550	**7 900**	**9 600**	*5 300*	*12 100*
trans-[L^{14}CoNCRu(CN)$_5$]$^-$	**26 300**	929	−757	**13 600**	**12 700**	*7 400*	*24 000*

[a] *vs.* Ag/AgCl. [b] Calculated from $\Delta E^oF/11.97$. [c] Calculated from eqn. (1). [d] Estimated from spectra (see text). [e] From eqn. (2) using estimated $\Delta\bar{\nu}_{1/2,app}$.

to the coordination sphere ultimately leads to a low spin d^7 ground state.[29–31] Given that, in the absence of an MMCT transition, the Co^{II} centers are the only possible chromophores in this region, the differences in the visible spectra of *trans*-[L^{14}CoNCRu(CN)$_5$]$^{2-}$ and *trans*-[L^{14S}CoNCFe(CN)$_5$]$^{2-}$ point to a spin state change where the former has a high spin Co^{II} centre while the latter has a low spin d^7 ground state. The d–d electronic absorption bands of high spin Co^{II} hexaamines are invariably very weak ($\varepsilon < 20$ dm^3 mol^{-1} cm^{-1})[32,33] and we would be unable to resolve any peaks of this intensity given the limitations of our equipment. By contrast, the putative Co^{II} spectral features of *trans*-[L^{14S}CoNCFe(CN)$_5$]$^{2-}$ are much more prominent and similar in both energy and intensity to other mixed donor (N,S) low spin Co^{II} complexes.[34]

Table 1 summarises the relevant spectroscopic and electrochemical data for these complexes. E_{op} and ΔG^o have been determined directly from the MMCT energy and the redox potential separation respectively, and the reorganisational energy (λ) has been calculated using eqn. (1), and the values relevant to this equation appear in bold type. In principle, λ may be determined independently of E_{op} and ΔG^o using eqn. (2), but an accurate measurement of the MMCT bandwidth ($\Delta\bar{\nu}_{1/2}$) is crucial given that λ is proportional to the square of the bandwidth *i.e.* error propagation will be large if a poor estimate of $\Delta\bar{\nu}_{1/2}$ is made. In all of the spectra shown in Fig. 4, the MMCT transition overlaps with d–d bands from the Co^{III} chromophore so an accurate measurement of $\Delta\bar{\nu}_{1/2}$ is not possible. Spectral deconvolution techniques may be applied assuming Gaussian band shapes. However, this introduces a potentially major systematic error if more than one combination of bands matches the experimental spectrum *i.e.* one is forced to choose the 'correct' MMCT bandwidth from two or more values of $\Delta\bar{\nu}_{1/2}$ derived from different deconvolution solutions. A further complication arises from spin orbit coupling[35] in the excited state, which may split the MMCT transition; leading to band asymmetry and broadening depending on the magnitude of the coupling constant. This is most significant in second and third row transition elements *i.e.* the MMCT band of *trans*-[L^{14}CoNCRu(CN)$_5$]$^-$ will be broadened more than *trans*-[L^{14}CoNCFe(CN)$_5$]$^-$ or *trans*-[L^{14S}CoNCFe(CN)$_5$]$^-$. Therefore, eqn. (2) only provides an upper bound for λ in the complexes discussed herein.‡

Inspection of Table 1 reveals that the dominant contributor to the observed variations in MMCT energy across the series is ΔG^o. The similar values of λ (Table 1) for the three complexes is consistent with the structural and electronic homology between these compounds. Outer sphere (solvent) reorganisational energies should be similar and, since all complexes bear isoelectronic low spin d^6–d^6 ground states, inner sphere reorganisational energies (coordinate bond length changes) should also be comparable.

Conclusions

Variations to donor or acceptor redox potentials of the cyano bridged mixed valence complex *trans*-[L^{14}Co^{II}NCFe^{III}(CN)$_5$]$^-$ have been achieved through metal substitution of the electron donor (Fe^{II} to Ru^{II}) or by ligand substitution at the electron acceptor (pentaamine L^{14} to amino-thioether L^{14S}). The ensuing changes to the MMCT energy could be rationalised quantitatively by application of Hush theory, and it was found that the free energy change between the redox isomers was the dominant effect in these systems. Reorganisational energies showed little variation, as one would expect given the structural and electronic similarities between the compounds.

‡ To illustrate this point we have estimated values of the bandwidth ($\Delta\bar{\nu}_{½,app}$) in the following way. In *trans*-[L^{14}CoNCFe(CN)$_5$]$^-$ and *trans*-[L^{14S}CoNCFe(CN)$_5$]$^-$, the lower energy half of the MMCT band (the lowest energy transition) should not overlap with any other band; enabling an estimate of $\Delta\bar{\nu}_{½}$ and hence λ_{app} (Table 1, italics). For *trans*-[L^{14}CoNCRu(CN)$_5$]$^-$ the MMCT band overlaps with the higher energy Co^{III} $^1A_{1g} \rightarrow {}^1T_{2g}$ transition (completely obscured) and the lower energy Co^{III} $^1A_{1g} \rightarrow {}^1T_{1g}$ band. Therefore, the apparent MMCT bandwidth ($\Delta\bar{\nu}_{½,app}$) is exaggerated, and the calculated value of λ (~24,000 cm^{-1}) is unrealistically large.

Acknowledgements

The Australian Research Council (project A10027090), the Australian Institute for Nuclear Science and Engineering (project 01/006) and Ministerio de Ciencia y Tecnología (project BQU2001-3205) are thanked for financial support of this work.

References

1 P. V. Bernhardt and M. Martinez, *Inorg. Chem.*, 1999, **38**, 424–5.
2 P. V. Bernhardt, B. P. Macpherson and M. Martinez, *Inorg. Chem.*, 2000, **39**, 5203–8.
3 P. V. Bernhardt, B. P. Macpherson and M. Martinez, *J. Chem. Soc., Dalton Trans.*, 2002, 1435–41.
4 P. V. Bernhardt, F. Bozoglian, B. P. Macpherson, M. Martinez, G. Gonzalez and B. Sienra, *Eur. J. Inorg. Chem.*, 2003, 2512–8.
5 M. B. Robin and P. Day, *Adv. Inorg. Chem. Radiochem.*, 1967, **10**, 247–422.
6 N. S. Hush, *Prog. Inorg. Chem.*, 1967, **8**, 391–444.
7 R. A. Krause and V. Carol, *Inorg. Chim. Acta*, 1986, **113**, 161–2.
8 G. A. Lawrance, M. Martinez, B. W. Skelton and A. H. White, *Aust. J. Chem.*, 1991, **44**, 113–21.
9 L. J. Farrugia, *J. Appl. Crystallogr.*, 1999, **32**, 837–8.
10 G. M. Sheldrick, *SHELX97—Programs for Crystal Structure Analysis (Release 97-2)*, Institut für Anorganische Chemie, Universität Göttingen, Germany, 1998.
11 L. J. Farrugia, *J. Appl. Crystallogr.*, 1997, **30**, 565.
12 A. W. Adamson and E. Gonick, *Inorg. Chem.*, 1963, **2**, 129–32.
13 A. J. Miralles, R. E. Armstrong and A. Haim, *J. Am. Chem. Soc.*, 1977, **99**, 1416–20.
14 I. Krack and R. van Eldik, *Inorg. Chem.*, 1989, **28**, 851–5.
15 M. Martinez, M.-A. Pitarque and R. van Eldik, *Inorg. Chim. Acta*, 1997, **256**, 51–9.
16 R. E. Hester and E. M. Nour, *J. Chem. Soc., Dalton Trans.*, 1981, 939–41.
17 C. Wang, B. K. Mohney, R. D. Williams, V. Petrov, J. T. Hupp and G. C. Walker, *J. Am. Chem. Soc.*, 1998, **120**, 5848–9.
18 G. A. Lawrance, T. M. Manning, M. Maeder, M. Martinez, M. A. O'Leary, W. C. Patalinghug, B. W. Skelton and A. H. White, *J. Chem. Soc., Dalton Trans.*, 1992, 1635–41.
19 T. W. Hambley, G. A. Lawrance, M. Martinez, B. W. Skelton and A. H. White, *J. Chem. Soc., Dalton Trans.*, 1992, 1643–8.
20 G. Wei, C. C. Allen, T. W. Hambley, G. A. Lawrance and M. Maeder, *Inorg. Chim. Acta*, 1997, **261**, 197–200.
21 P. V. Bernhardt and B. P. Macpherson, *Acta Crystallogr., Sect. C*, 2003, **59**, m533–m6.
22 P. V. Bernhardt and B. P. Macpherson, *Acta Crystallogr., Sect. C*, 2003, **59**, m467–m70.
23 H. J. Meyer and J. Pickardt, *Acta Crystallogr., Sect. C*, 1988, **44**, 1715–17.
24 D. F. Mullica and E. L. Sappenfield, *Inorg. Chim. Acta*, 1997, **258**, 101–4.
25 D. F. Mullica, P. K. Hayward and E. L. Sappenfield, *Inorg. Chim. Acta*, 1996, **253**, 97–101.
26 D. F. Mullica, P. K. Hayward and E. L. Sappenfield, *Inorg. Chim. Acta*, 1996, **244**, 273–6.
27 H. W. Kang, G. Moran and E. Krausz, *Inorg. Chim. Acta*, 1996, **249**, 231–5.
28 F. M. Crean and K. Schug, *Inorg. Chem.*, 1984, **23**, 853–7.
29 R. V. Dubs, L. R. Gahan and A. M. Sargeson, *Inorg. Chem.*, 1983, **22**, 2523–7.

30 J. A. Hartman, E. J. Hintsa and S. R. Cooper, *J. Am. Chem. Soc.*, 1986, **108**, 1208–14.
31 T. M. Donlevy, L. R. Gahan and T. W. Hambley, *Inorg. Chem.*, 1994, **33**, 2668–76.
32 I. I. Creaser, R. J. Geue, J. M. Harrowfield, A. J. Herlt, A. M. Sargeson, M. R. Snow and J. Springborg, *J. Am. Chem. Soc.*, 1982, **104**, 6016–25.
33 P. V. Bernhardt and L. A. Jones, *Inorg. Chem.*, 1999, **38**, 5086–90.
34 T. M. Donlevy, L. R. Gahan, T. W. Hambley and R. Stranger, *Inorg. Chem.*, 1992, **31**, 4376–82.
35 E. M. Kober, K. A. Goldsby, D. N. S. Narayana and T. J. Meyer, *J. Am. Chem. Soc.*, 1983, **105**, 4303–9.